Frequency-modulated atomic force spectroscopy on NiAl(110) partially covered with a thin alumina film

M. Heyde,* M. Kulawik, H.-P. Rust, and H.-J. Freund
Fritz-Haber-Institut der Max-Planck-Gesellschaft, Faradayweg 4-6, D-14195 Berlin, Germany
(Received 13 December 2005; published 15 March 2006)

Force spectroscopy has been performed using a low-temperature scanning tunneling microscope (STM) and atomic force microscope (AFM) with small amplitude frequency modulation (FM). Frequency shift versus distance curves acquired on NiAl(110) are compared to measurements performed on a thin alumina film. Interaction force and energy are determined from the frequency shift. Due to the high stability of small amplitude frequency modulation in combination with a stiff force sensor, it is possible to observe clear differences in the interaction potential between the metal and oxide surface. The setup also allows us to gain specific information in the repulsive regime of the contact formation, where elastic and plastic stages have been identified.

DOI: 10.1103/PhysRevB.73.125320 PACS number(s): 68.37.Ps, 68.47.De, 68.47.Gh, 62.20.−x

I. INTRODUCTION

Several groups have presented images with atomic resolution by frequency-modulation atomic force microscopy (FM-AFM) on different materials.[1–4] However, proper descriptions of the tip-sample interaction and contrast mechanisms are still under discussion. The understanding of these issues leads toward a microscopy of specific surface properties and an extension of FM-AFM beyond topography measurements. Many strategies have been developed to add information on chemical and physical properties to scanning probe microscopy methods, like inelastic tunneling spectroscopy,[5] electron-spin resonance,[6] or combined time-of-flight scanning force microscopy.[7] Quantitative measurements of tip-sample interaction by FM-AFM spectroscopy enable one to distinguish between different surface species.[8–12] The forces involved in imaging are probed as a function of relative distance between tip and sample, with different surface species expected to have different characteristics. The interaction force between tip and sample is composed of many contributions, like electrostatic, magnetic, van der Waals, and chemical forces in ultrahigh vacuum (UHV). For high sensitivity to short range chemical forces, it is desirable to filter out long range force contributions. Long range electrostatic forces can be minimized by compensating the contact potential difference with the sample voltage.[13] Magnetic forces can be avoided by choosing magnetically insensitive tip materials. The elimination of van der Waals forces is experimentally not possible. For the enhancement of short range contribution in FM-AFM, the oscillation amplitude of the cantilever plays a major role. In classical FM-AFM, empirically found parameters have been used, which are currently referred to as large oscillation amplitudes. A spring constant of $k=17$ N/m, an eigenfrequency of $f_0=114$ kHz, a frequency shift of $\Delta f=-60$ Hz, and an amplitude of $A=40$ nm are typical values to obtain atomic resolution.[2] This means that the atomically resolved imaging contrast induced by chemical binding forces with the length scale of about 0.2 nm is probed with oscillation amplitudes, which are several hundred times larger. The idea to use smaller amplitudes in FM-AFM imaging has been pioneered by Giessibl.[14–16] Calculations[17] predict an increased sensitivity for chemical short range forces and reduced noise when using smaller oscillation amplitudes in combination with stiffer cantilevers. With such a setup, atomically resolved images of Si(111) with $k=1800$ N/m, $f_0=16.86$ kHz, $\Delta f=-160$ Hz, and $A=0.8$ nm and of KCl(001) with $k=1800$ N/m, $f_0=14.77$ kHz, $\Delta f=-4$ Hz, and $A=0.9$ nm have been obtained.[14,18] Such imaging as well as force spectroscopy measurements by King *et al.*[19] are referenced as FM-AFM experiments performed with small oscillation amplitudes. Recent theoretical studies have emphasized the use of even smaller oscillation amplitudes in FM-AFM.[20] The amplitudes should be smaller than the shortest interaction length scale of interest. This highlights the road map for future experiments to improve image resolution and increase the sensitivity of force spectroscopy to chemical short range interactions. Here, we present detailed FM-AFM spectroscopy measurements performed with oscillation amplitudes in the range of $A=0.4$ nm at surfaces with different chemical composition.

II. EXPERIMENT

High stability of the experimental setup is needed for the detailed investigation of short range forces, which can be achieved at cryogenic temperatures. At low temperatures, the thermal drift of the microscope setup as well as piezodrift, hysteresis, and creep is reduced. Furthermore, enhanced stability of atomic configuration at the tip end is achieved, which prevents sudden jumps of the foremost tip atoms. All measurements presented in this publication were performed in UHV, using a custom-built microscope operated at 5 K.[21] The setup allows the simultaneous acquisition of the tunneling current in combination with FM detection. The sensor is operated by the sensor controller/FM-detector easyPLLplus from Nanosurf[22] in the self-exciting oscillation mode.[23] An additional custom-built analog FM detector has been used for the frequency shift recording based on Ref. 24. A schematic setup of the AFM using the FM technique is shown in Fig. 1. The spring system in our experimental setup is a self

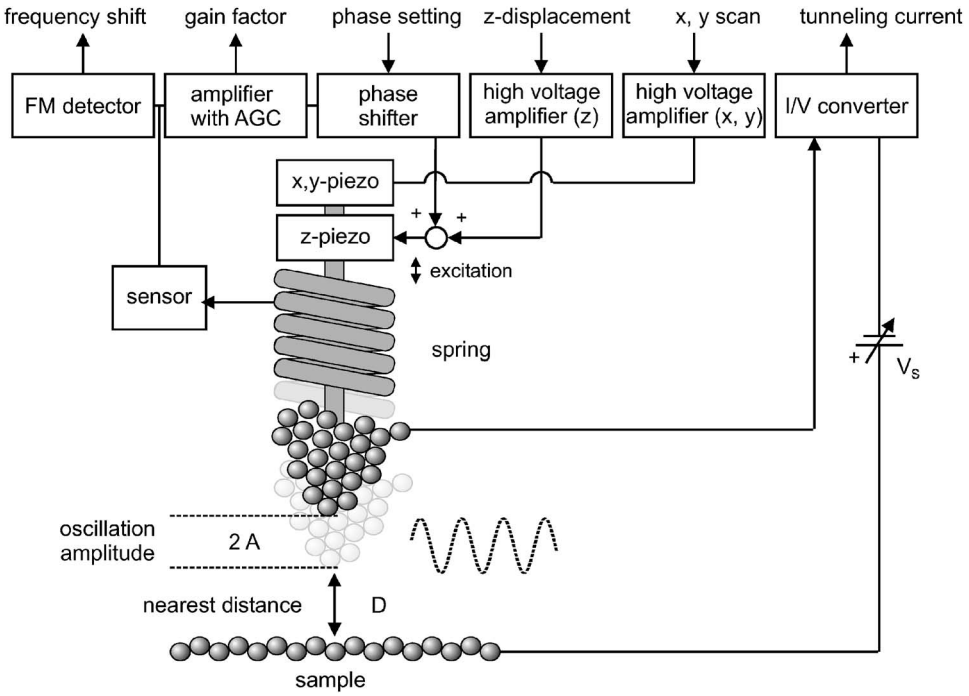

FIG. 1. Schematic setup of the FM-AFM and STM operated in UHV. Definition of parameters: the tip oscillates with amplitude A and the nearest distance between tip apex and sample surface is D.

sensing double quartz tuning fork,[21] which has a resonance frequency of $f_0=17.44$ kHz, a Q-factor of 12 500, and a stiffness of about $k=30\,000$ N/m. Details of the calibration procedure of the spring constant are given in Sec. III. The force constant is significantly higher than typical interatomic force constants. This prevents a sudden "jump-to-contact" of the cantilever even at very small tip-sample distances. Also, the often observed breakdown and instability of amplitude oscillation after contact formation in the repulsive regime is reduced. The force sensor is operated at constant oscillation amplitude in the range of about $A=0.4$ nm. The detected oscillation amplitude signal is fed into an automatic gain control (AGC) circuit and is used to excite the double tuning fork mechanically by the z-piezo. A phase shifter ensures that the spring system is excited at its resonance frequency. This operating mode of constant oscillation amplitude allows one to probe the regime of strong repulsive force in contrast to an operation mode at a constant excitation amplitude, where the oscillation amplitude decays as the vibrating tip penetrates the repulsive interaction regime.[25] A cut Pt/Ir wire with a diameter of 0.25 mm is used as a tip. The tip is electrically connected by a thin Pt/Rh wire with a diameter of 50 μm. Both tip and Pt/Rh wire are insulated from the tuning fork electrodes to avoid crosstalk between the tunneling current and the amplitude detection.

The analysis of thin oxide films is of great interest for research.[26–29] The use of thin oxide films ranges from insulating films in semiconductor devices to protective films against corrosion and mechanical wear. Here we have started a detailed FM-AFM spectroscopy analysis of NiAl(110) and a thin alumina film grown on that metal surface, which serves as a model system in catalysis.[30–32] The oxide consists of two Al-O layers and is approximately 0.5 nm in height. Its band gap of 8 eV is slightly smaller than that of bulk alumina. The NiAl(110) surface was cleaned by repeated cycles of Ar^+ sputtering and annealing to 1000 °C. Afterwards, the thin oxide film was prepared by dosing O_2 at 280 °C and subsequent annealing to 800 °C.[30] For a partially covered thin oxide film the dosing time of O_2 needs to be reduced. A full oxidation of the NiAl surface is obtained by dosage of 1200 L O_2. If the latter is reduced to 200 L, the surface contains both areas of alumina and of bare NiAl. Figure 2 shows a NiAl sample which is partially oxidized. On the right side, the pristine NiAl can be distinguished, which exhibits a modulation of the local density of states.[33] On the left side of the image, the alumina film is visible. Alumina grows on NiAl(110) in two reflection domains, denoted A and B. The unit cell of the two domains has been marked in Fig. 2. The surface contrast in Fig. 2 allows a clear determination of the metal and the oxide film sites.

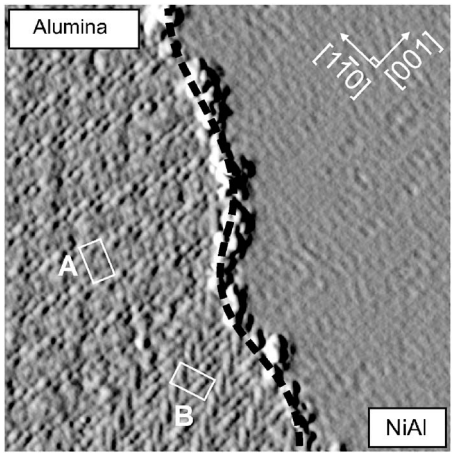

FIG. 2. STM image of NiAl(110) substrate partially covered by alumina. The unit cells of the two domains of the thin oxide film are marked by A and B in reference to the orientation of NiAl(110). A dashed line marks the decorated border, between the oxide film and the metal substrate. Scan size 20 nm × 20 nm, $I_t=0.025$ nA, $V_{\text{sample}}=-500$ mV.

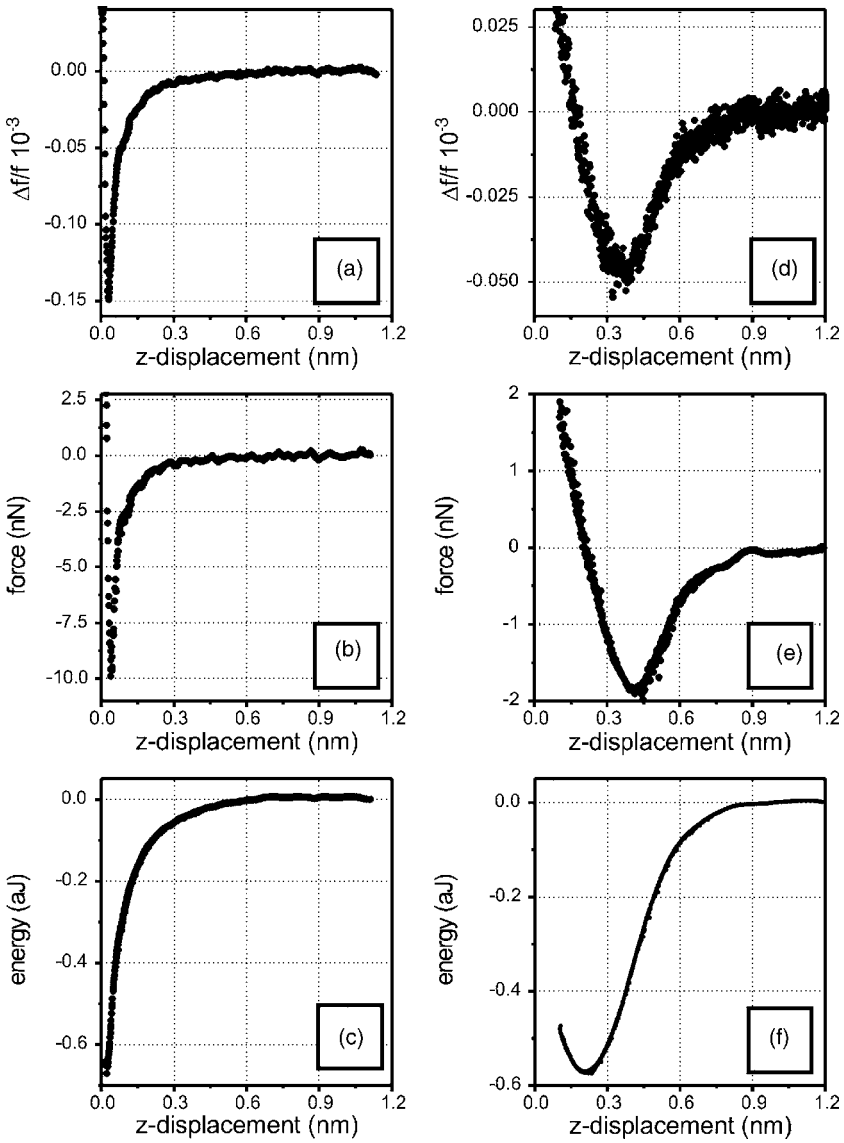

FIG. 3. The measured data [(a), (d)] have been obtained in UHV at 5 K. $V_{sample}=0$ mV. (a) $\Delta f(z)$ curve recorded on NiAl(110), (b) recovered force of [(a), (c)] recovered energy of [(a), (d)] $\Delta f(z)$ curve recorded on thin alumina film, and (e) recovered force of [(d), (f)] recovered energy of (d).

III. RESULTS AND DISCUSSION

In order to characterize the tip-sample interaction with small oscillation amplitude FM-AFM spectroscopy, we have measured frequency shift versus distance curves on the NiAl(110) surface and on areas covered with the thin alumina film. Typical curves of the tip approach on the metal and the oxide film are shown in Figs. 3(a) and 3(d), respectively. The characteristics of the frequency shift close to the surface differ significantly for NiAl(110) and alumina film. Comparing the two curves in the region where the attractive force increases with decreasing distance, it can be seen that the slope of the interaction is steeper on the metal than on the oxide surface. Following an initial slow variation of the interaction between the NiAl(110) substrate and the tip, we observe a sharp increase in the attractive regime between the tip and sample close to the minimum. The onset of the large attractive interaction seems to occur in a near-contact region indicated by a large tunneling current of several nA when a small tunneling voltage is applied. In such metallic systems, wetting is possible, where the sample can be wet by the tip or vice versa. The bond formation between tip and sample atoms results in relaxation of the positions of the foremost atoms in the tip and sample at small separations. A wetting results in an adhesive contact formation between the two surfaces. An adhesion-induced partial wetting can occur.[34] The contact formation in metallic systems is driven by the tendency of the atoms at the interfacial regions of the tip and sample to optimize their embedding energies. On the alumina film the onset of the attractive region is very smooth and no sharp increase in the tip-sample interaction is observed [Fig. 3(d)]. The absence of kinks and steps gives rise to the assumption that the curves recorded on the oxide film are dominated by elastic tip-sample interactions. To determine the interaction force $F(z)$ between tip and sample as well as the according energy $U(z)$, formulas (1) and (2) are used.[35] These formulas allow a determination of $F(z)$ and $U(z)$ from the frequency shift, and are also valid for our oscillation amplitude. The expression for the force in terms of the frequency shift is given by

$$F(D) = \frac{2k}{f_0}\int_D^\infty \Delta f(z)\left[\left(1 + \frac{A^{1/2}}{8\sqrt{\pi(z-D)}}\right) - \frac{A^{3/2}}{\sqrt{2(z-D)}}\frac{d}{dz}\right]dz, \tag{1}$$

where D the distance of closest approach between tip and sample, z is the tip-sample distance, and F is the interaction force between tip and sample. The definition of the parameters D and A is illustrated in Fig. 1. Integrating Eq. (1) gives the corresponding expression for the interaction energy $U(D)$ between tip and sample

$$U(D) = \frac{2k}{f_0}\int_D^\infty \Delta f(z)\left((z-D) + \frac{A^{1/2}}{4}\sqrt{\frac{z-D}{\pi}} + \frac{A^{2/3}}{\sqrt{2(D-z)}}\right)dz. \tag{2}$$

Figure 3 shows the recovered force [(b), (e)] and energy curves [(c), (f)] which were calculated after smoothing the frequency shift versus z-displacement curves [(a), (d)]. The minimum values of the recovered force and energy on the metallic surface is $F=-9.6$ nN and $U=-0.67$ aJ (-4.2 eV), respectively. For the oxide film, the recovered force is $F=-1.9$ nN and the recovered energy is $U=-0.57$ aJ (-3.6 eV). The purely repulsive regime of the force distance curves has been fitted using a linear force law. This leads to a calculated contact stiffness for the NiAl(110) and the alumina film of 500 and 10 N/m, respectively. This result shows that the alumina film is much softer than the NiAl(110) metal surface. However, in case of the NiAl(110) the force contribution in the repulsive regime is dominated by structural rearrangements and plastic deformations. The determined force and energy values are well in range with other experimentally obtained FM-AFM measurements.[13,36] It is difficult to determine whether the measured chemical force and energy involve more than just a single pair of atoms. Even for an atomically sharp tip, there can be more than one bond interaction between the tip and the surface in the near-contact region, such as shown by calculations.[37] However, quantitative modeling of specific tip-sample interactions relies on parameters which cannot be determined easily in experiment. For example, the tip radius and its actual separation from the surface are not known. Also the chemical composition of the tip apex is usually unknown. However, this effects the tip-sample interaction significantly and can even reverse the imaging contrast of FM-AFM in the case of a tip change.[38]

In the following, the accuracy of the data presented in Figs. 3(b), 3(c), 3(e), and 3(f) is evaluated, which is determined by the accuracy of k and A. To determine k, one possible solution in cantilever calibration is to add a known mass to the cantilever and to observe the shift in resonant frequency.[39] Such experiment has been performed by adding a grinded carbide sphere to a double tuning fork test assembly. The determined force constant is $k=30\,000$ N/m. This value is also in good agreement with finite element calculations.[40] However, Eqs. (1) and (2) show that k only influences the absolute values, but not the shape of the force or energy curve, while the small oscillation amplitude A directly influences the shape of the recovered curves. The oscillation amplitude A was calibrated by measuring the variation of the z-displacement as a function of the applied dither oscillation amplitude at a mean constant tunneling current as a reference signal. The measured tunneling current is given by an average over several oscillation cycles, due to the bandwidth of the tunneling current-preamplifier, which is much smaller than the oscillation frequency f_0. The gradient in the linear part of the curve has been used to calculate the calibration factor of 8 pm/mV$_{\mathrm{rms}}$.

Plotting frequency shift versus z-displacement curves of the approach and the retraction provides further insight into chemical bond and contact formation of tip/metal and tip/oxide, respectively. The interaction force experienced by the tip upon approach and retraction may be different if plastic deformation takes place. Figures 4(a) and 4(b) show the frequency shift versus z-displacement for the approach and the retraction on the metallic surface while Figs. 4(c) and 4(d) show the curves obtained on the oxide film. The process in which the tip penetrates the surface involves transition from elastic to plastic behavior of the NiAl(110). Upon indentation and retraction, the step marked by A in Figs. 4(a) and 4(b) indicates a reversible stage due to the reconfiguration at the same tip-sample distance. The series of consecutive steps marked by B indicates irreversible deformations during the withdrawal of the tip from the sample surface. The physical phenomena that are responsible for the qualitative shape of the indentation curves can be understood by molecular dynamic simulations.[41] For the metallic surface, the tip-sample interaction during the acquisition of the z-displacement causes significant plastic deformation, involving ductile extension, formation of connective neck of atomic dimensions, and rupture. The hysteresis in the frequency shift versus distance curve in Fig. 4(a) between lowering and lifting the tip suggests the formation of an extended neck.[34] The elongation exhibits straining and yielding stages, which are reflected in the steps of the recorded curve during retraction. The elongation mechanism consists of a sequence of elastic and plastic stages accompanied by atomic structural rearrangement shown in more detail in Fig. 4(b). The contact formation leads to an adhesion hysteresis, which is structurally irreversible, so that different hysteresis are observed every time the tip is retracted. Such adhesive forces have been predicted and observed for different types of materials of tip and sample in metallic systems.[41–44] Many molecular dynamic simulations of deformable metal tips indenting metal surfaces have shed light on the physical phenomena that are involved in adhesive interactions, their results reproduce nicely our experiments preformed on the metallic NiAl(110).

The curves obtained on the thin alumina film reveal a different behavior. The tip-sample interaction for the oxide film indicates no instabilities and no significant plastic deformations in the probed interaction regime. Here, we observe neither steps nor kinks or hysteresis effects upon indentation and separation of tip and sample. The oxide surface is not modified by plastic deformations, clearly seen by the nearly identical curves obtained for the approach and the retraction in Figs. 4(c) and 4(d). This indicates that relaxation and wetting effects are much weaker for the tip interacting with the alumina film than compared to the same tip interacting with

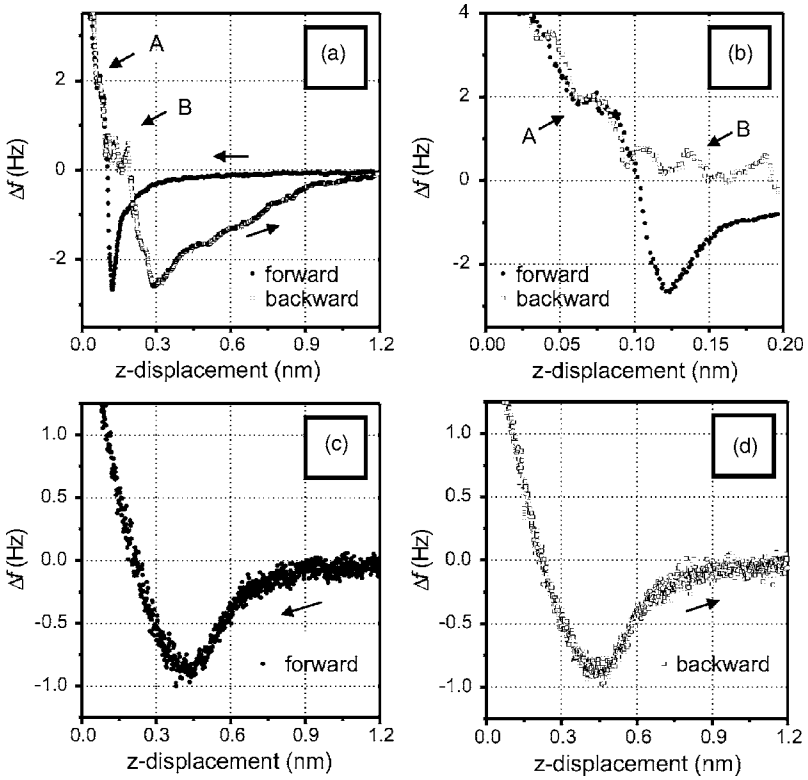

FIG. 4. Frequency shift versus z-displacement curves obtained in UHV at 5 K on NiAl(110) [(a), (b)] and thin alumina film [(c), (d)]. The black circles mark the approach and the white rectangles the retraction between tip and sample. In (b) an enlargement of (a) is given, where elastic (A) and plastic (B) stages accompanied by atomic structural rearrangement are marked.

the NiAl(110). The nonadhesive interaction of the alumina film is not unexpected since aluminum oxide is chemically fairly inert. The curve shape observed on the thin alumina film is qualitatively in good agreement with molecular dynamic simulations of covalent and ionic systems. Harrison *et al.*[45] have simulated the indentation of a diamond(111) substrate, where they also found an elastic and nonadhesive indentation mechanism. Initial and final state of the tip-sample geometry were identical. No hysteresis in the tip-sample interaction was observed until a maximum load of about 200 nN. Only further increasing of the load lead to plastic deformations resulting in adhesion between tip and surface. The adhesion during the indentation was found to depend on the maximum value of the applied load.

In Fig. 5 images before (a) and after (b) the acquisition of frequency shift versus z-displacement curves are shown in order to support the interpretation of the curves plotted in Fig. 4. It can be seen that the oxide film remains unchanged at small loads while the metal surface is modified. This also explains why it is for some samples possible to obtain images in repulsive mode as presented, for example, by Giessibl *et al.* on CaF_2 (Ref. 16) and our group on MgO.[46] Tip-sample interaction on oxide films exhibits for small interaction forces rather elastic than plastic deformation. Such an inert tip-sample interaction at the beginning of the repulsive regime allows stabilization of the feedback to a constant repulsive interaction. Further details can be found in Ref. 46. The significant difference in the obtained FM-AFM spectroscopy curves has also a consequence for the imaging process. The lateral variation of the strong chemical short range interaction affects the tip-sample distance, when imaging at a constant frequency shift. This can lead to incorrect apparent heights in FM-AFM measurements on heterogeneous surfaces and needs further analysis.

IV. CONCLUSION

We have investigated a metallic NiAl(110) surface and a thin alumina film by small amplitude force spectroscopy. The quality of the presented curves clearly shows the advantages of using high force constants in combination with small oscillation amplitudes. Frequency shift, recovered force, and recovered energy versus z-displacement have been obtained for the bare metal surface and the thin alumina film. Curves recorded from the metal surface show a clear difference to those recorded on the oxide film. In the repulsive regime, elastic and plastic stages with atomic rearrangements have been identified on the NiAl. Different types of bond and contact formation have been found for metal and oxide.

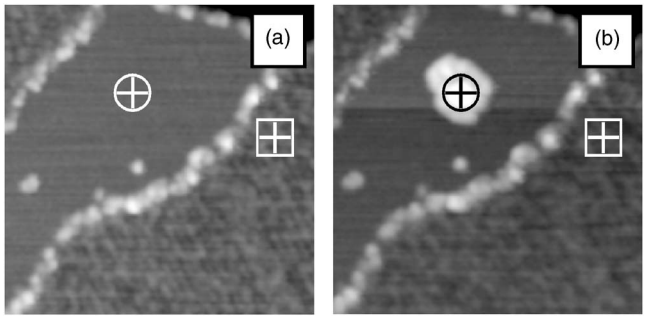

FIG. 5. STM images of NiAl(110) substrate partially covered with alumina before (a) and after (b) the acquisition of frequency shift versus z-displacement curves. A cross surrounded by a square marks the tip position on the oxide and a cross surrounded by a circle marks the tip position on the metal, where spectroscopy curves have been obtained consecutively. Scan size 27 nm $\times$ 27 nm, I_t=0.01 nA, V_{sample}=50 mV, and T=5 K.

ACKNOWLEDGMENTS

It is a pleasure for M.H. to acknowledge useful discussions with U. D. Schwarz (Yale University) and Hendrik Hölscher (University Münster, Germany). We thank W. Matthees for his contribution of the finite element simulations. Also many thanks to J. E. Sader (University of Melbourne, Australia) for providing the MATHEMATICA code for implementing formulas (1) and (2). Financial support from the Studienstiftung des deutschen Volkes is gratefully acknowledged (M.K.).

*Electronic address: heyde@fhi-berlin.mpg.de

[1] F. J. Giessibl, Science **267** 68 (1995).
[2] K. S. Kitamura and M. Iwatsuki, Jpn. J. Appl. Phys., Part 2 **34**, L145 (1995).
[3] W. Allers, A. Schwarz, U. D. Schwarz, and R. Wiesendanger, Rev. Sci. Instrum. **69**, 221 (1998).
[4] M. Bammerlin, R. Lüthi, E. Meyer, A. Baratoff, J. Lü, M. Guggisberg, C. Loppacher, C. Gerber, and H.-J. Güntherodt, Appl. Phys. A: Mater. Sci. Process. **66**, S293 (1998).
[5] B. C. Stipe, M. A. Rezaei, and W. Ho, Science **280**, 1732 (1998).
[6] C. Durkan and M. E. Welland, Appl. Phys. Lett. **80**, 458 (2002).
[7] D. Lee, A. Wetzel, R. Bennewitz, E. Meyer, M. Despont, P. Vettiger, and C. Gerber, Appl. Phys. Lett. **84**, 1558 (2004).
[8] B. Gotsmann, B. Anczykowski, C. Seidel, and H. Fuchs, Appl. Surf. Sci. **140**, 314 (1999).
[9] H. Hölscher, W. Allers, U. D. Schwarz, A. Schwarz, and R. Wiesendanger, Phys. Rev. Lett. **83**, 4780 (1999).
[10] U. Dürig, Appl. Phys. Lett. **75**, 433 (1999).
[11] M. A. Lantz, H. J. Hug, R. Hoffmann, P. J. A. van Schendel, P. Kappenberger, S. Martin, A. Baratoff, and H.-J. Gýntherodt, Science **291**, 2580 (2001).
[12] C. L. Pang, T. V. Ashworth, H. Raza, S. A. Haycock, and G. Thornton, Nanotechnology **15**, 862 (2004).
[13] M. Guggisberg, M. Bammerlin, C. Loppacher, O. Pfeiffer, A. Abdurixit, V. Barwich, R. Bennewitz, A. Baratoff, E. Meyer, and H. J. Güntherodt, Phys. Rev. B **61**, 11151 (2000).
[14] F. J. Giessibl, Appl. Phys. Lett. **76**, 1470 (2000).
[15] S. Hembacher, F. J. Giessibl, J. Mannhart, and C. F. Quate, Phys. Rev. Lett. **94**, 056101 (2005).
[16] F. J. Giessibl and M. Reichling, Nanotechnology **16**, S118 (2005).
[17] F. J. Giessibl, H. Bielefeldt, S. Hembacher, and J. Mannhart, Appl. Surf. Sci. **140**, 352 (1999).
[18] F. J. Giessibl, Rev. Mod. Phys. **75**, 949 (2003).
[19] G. M. King, J. S. Lamb, and G. Nunes, Appl. Phys. Lett. **79**, 1712 (2001).
[20] J. E. Sader and S. P. Jarvis, Phys. Rev. B **70**, 012303 (2004).
[21] M. Heyde, M. Kulawik, H.-P. Rust, and H.-J. Freund, Rev. Sci. Instrum. **75**, 2446 (2004).
[22] Nanosurf AG, Grammetstrasse 14, CH-4410 Liestal, Switzerland.
[23] K. Kobayashi, H. Yamada, H. Itoh, T. Horiuchi, and K. Matsushige, Rev. Sci. Instrum. **72**, 4383 (2001).
[24] T. R. Albrecht, P. Grütter, D. Horne, and D. Rugar, J. Appl. Phys. **69**, 668 (1991).
[25] B. Gotsmann and H. Fuchs, Appl. Surf. Sci. **188**, 355 (2002).
[26] C. T. Campbell, Surf. Sci. Rep. **27**, 1 (1997).
[27] H.-J. Freund, Faraday Discuss. **114**, 1 (1999).
[28] M. Bäumer and H.-J. Freund, Prog. Surf. Sci. **61**, 127 (1999).
[29] W. T. Wallace, B. K. Min, and D. W. Goodman, Top. Catal. **34**, 17 (2005).
[30] R. M. Jaeger, H. Kuhlenbeck, H. J. Freund, M. Wuttig, W. Hoffmann, R. Franchy, and H. Ibach, Surf. Sci. **259**, 235 (1991).
[31] M. Kulawik, N. Nilius, H.-P. Rust, and H.-J. Freund, Phys. Rev. Lett. **91**, 256101 (2003).
[32] G. Kresse, M. Schmid, E. Napetschnig, M. Shishkin, L. Köhler, and P. Varga, Science **308**, 1440 (2005).
[33] Z. Song, J. I. Pascual, H. Conrad, K. Horn, and H.-P. Rust, Appl. Phys. A: Mater. Sci. Process. **72**, S159 (2001).
[34] U. Landman and W. D. Luedtke, J. Vac. Sci. Technol. B **9**, 414 (1991).
[35] J. E. Sader and S. P. Jarvis, Appl. Phys. Lett. **84**, 1801 (2004).
[36] A. Schirmeisen, G. Cross, A. Stalder, P. Grütter, and U. Dürig, Appl. Surf. Sci. **157**, 274 (2000).
[37] S. H. Ke, T. Uda, R. Perez, I. Stich, and K. Terakura, Phys. Rev. B **60**, 11631 (1999).
[38] A. Schwarz, W. Allers, U. D. Schwarz, and R. Wiesendanger, Phys. Rev. B **61**, 2837 (2000).
[39] J. P. Cleveland, S. Manne, D. Bocek, and P. K. Hansma, Rev. Sci. Instrum. **64**, 403 (1993).
[40] W. Matthees (private communication).
[41] U. Landman, W. D. Luetdke, N. A. Burnham, and R. J. Colton, Science **248**, 454 (1990).
[42] N. Agraït, G. Rubio, and S. Vieira, Phys. Rev. Lett. **74**, 3995 (1995).
[43] G. Cross, A. Schirmeisen, A. Stalder, P. Grütter, M. Tschudy, and U. Dürig, Phys. Rev. Lett. **80**, 4685 (1998).
[44] V. Yakimov and R. Erlandsson, Rev. Sci. Instrum. **71**, 133 (2000).
[45] J. A. Harrison, C. T. White, R. J. Colton, and D. W. Brenner, Surf. Sci. **271**, 57 (1992).
[46] M. Heyde, M. Sterrer, H.-P. Rust, and H.-J. Freund, Appl. Phys. Lett. **87**, 083104 (2005).